$Na_{12}K_{18}In_{53}Tl_7$: a novel mixed In/Tl phase hierarchically related to the C15 Friauf–Laves structure type. Synthesis, crystal and electronic structure

David Flot, Monique Tillard-Charbonnel* and Claude Belin

Laboratoire des Agrégats Moléculaires et Matériaux Inorganiques (*CNRS ESA 5072*), *Université de Montpellier II, Sciences et Techniques du Languedoc, 2, Place Eugène Bataillon, 34095 Montpellier cédex 5, France*

Crystals of compound $Na_{12}K_{18}In_{53}Tl_7$ were first obtained by slow cooling of an alloy of nominal composition $Na_2K_2In_5Tl_3$ prepared by fusion of the elements in a niobium container. Once the composition of the crystal was determined, a new synthesis was carried out starting from the ideal composition, it yielded a homogeneous and well-crystallized product. Crystal structure has been established by means of X-ray single crystal diffraction techniques ($R\bar{3}m$, Z = 4, $a = b = 16.846(3)$, $c = 43.339(7)$ Å, $R_1 = 0.036$ and $wR2 = 0.085$, SHELXL) for 1462 independent reflections and 121 parameters varied. A few atomic sites have been found with mixed In/Tl occupations. The structure contains twelvefold and sixfold *exo*-bonded icosahedra and pairs of open 16-vertex polyhedra. This structure is hierarchically related to the C15 Friauf–Laves cubic structure type ($MgCu_2$), in which icosahedra and 16-vertex polyhedra would occupy the Cu and Mg positions, respectively. Structural relationship with other cubic and rhombohedral intermetallic phases of Group 13 elements has also been investigated. Chemical bonding within the cluster network has been analyzed by means of extended Hückel molecular orbital and band calculations. The compound has a closed shell bonding and semiconducting properties.

$Na_{12}K_{18}In_{53}Tl_7$: Une nouvelle phase mixte (In/Tl) dérivant du type structural C15 (Friauf–Laves). Synthèse, structure cristalline et structure électronique. Le composé $Na_{12}K_{18}In_{53}Tl_7$ a d'abord été isolé à partir d'un alliage de composition nominale $Na_2K_2In_5Tl_3$ préparé par fusion des éléments dans un container de niobium, suivie d'un lent refroidissement. Une fois la composition des cristaux déterminée avec précision, un lingot homogène et bien cristallisé a été préparé à la stoechiométrie idéale. La structure cristalline a été déterminée par diffraction X sur monocristal ($R\bar{3}m$, Z = 4, $a = b = 16{,}846(3)$, $c = 43{,}339(7)$ Å, $R_1 = 0{,}036$ et $wR_2 = 0{,}085$, SHELXL) pour 1462 réflexions indépendantes et 121 variables. Quelques sites atomiques présentent des occupations mixtes indium/thallium. La structure contient deux types d'icosaèdres hexa- et dodeca-coordinés aux polyèdres environnants, ainsi que des paires de polyèdres ouverts contenant 16 atomes. Elle est construite à partir de la structure type $MgCu_2$ (C15) où les positions des atomes de cuivre et de magnésium sont hiérarchiquement occupées par des icosaèdres et des polyèdres à 16 atomes. Des relations structurales entre ce composé et d'autres phases rhomboédriques et cubiques ont aussi été établies. La liaison chimique dans le réseau de clusters a été étudiée à l'aide de calculs d'orbitales moléculaires et de calculs de bandes (extended Hückel). Ce composé a une couche de valence remplie en accord avec ses propriétés semi-conductrices.

The remarkable richness and variety of clusters and cluster frameworks found in the intermetallic chemistry of alkali metals and Group 13 elements (particularly the Ga, In and Tl triad) has boosted our interest in understanding various problems such as stoichiometry, structure, chemical bonding and also in interpreting properties of these unusual compounds.

Although a few examples of discrete clusters have been reported,[1,2] gallium and indium display a general trend of forming extended anionic cluster frameworks, *i.e.* electron deficient metal aggregates that are generally interconnected through classical 2c–2e bonds resulting in electron-poor (delocalized bonding) and electron-precise (localized bonding) structural domains. On the other hand, thallium chemistry is very rich in isolated cluster moieties[3–5] reminiscent of boron chemistry.

Owing to the pronounced difference in electronegativity between alkali metals and Group 13 elements (triels), complete electron transfer to the triels is assumed in these intermetallic compounds. The simple Zintl concept for normal valence compounds may afford a preliminary comprehensive approach of chemical bonding therein. However, depending on the actual electron richness of the triel sublattice, bonding may deviate more or less from the 8-*N* rule and conform, or not, to the classical valence concept. In recent years, new insights into these problems have been provided based on fine crystal structure determinations,[2,6] electron counting procedures like those initiated by Wade,[7] as well as on more sophisticated quantum mechanical calculations.[8–16]

Electronic dependences have been exemplified in the Li–Ga system[6] in which the structures of six compounds have been determined crystallographically (Fig. 1). Gallium clustering within these anionic lattices is achieved as a function of the number of available electrons: gallium zig-zag chains in Li_2Ga,[17] puckered layers in Li_3Ga_2 [17] and Li_5Ga_4,[18] and 3D networks in LiGa (diamond lattice), Li_5Ga_9 [6] and Li_2Ga_7 (interconnected clusters).[19]

Using different sizes of alkali metals[6,20,21] may lessen cation packing limitations, allowing higher electron concentrations on the triel lattices and preventing formation of hypo-electronic (with regard to Wade's rules) clusters. Atomic

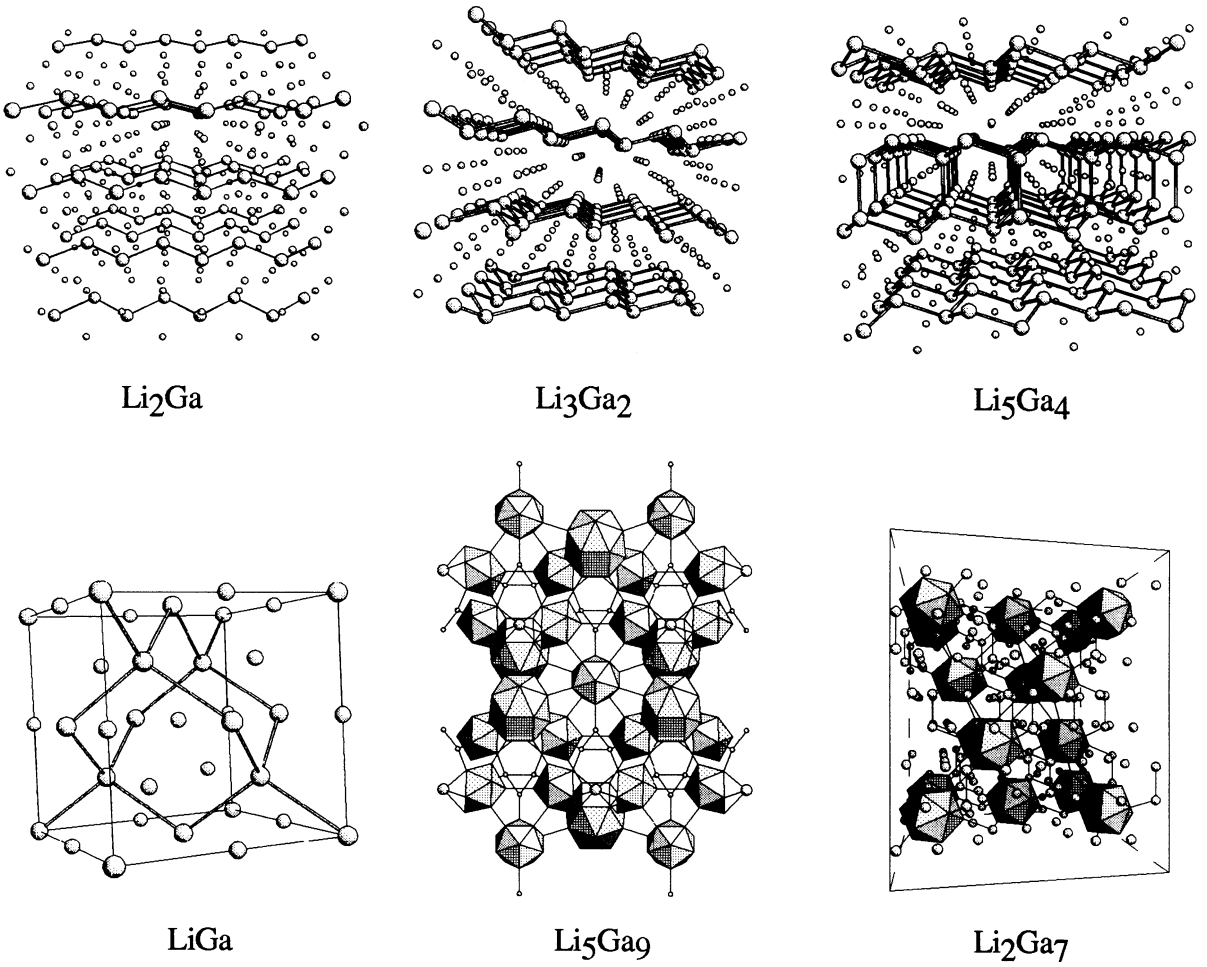

Fig. 1 Clustering and framework modelling in the binary Li–Ga system as a function of gallium reduction

defections may occur within more reduced anionic networks leading to *nido*, *arachno*, *etc.* open clusters.[6] These findings and other peculiarities observed in such systems highlight the strong versatility of this triad of elements to form various and intricate frameworks in which bonding and electronic requirements may still raise some questions.

In order to widen understanding, we have investigated the quaternary system Na–K–In–Tl. In this paper we describe the preparation and crystal structure of the $Na_{12}K_{18}In_{53}Tl_7$ phase. Its cluster network will be compared with those of closely related phases. Chemical bonding therein is analyzed on the basis of some extended Hückel molecular orbital and tight-binding band calculations.

Experimental

Indium and thallium (Fluka, respectively 99.95 and 99.99% pure) were used after their surfaces were scraped in a glove box (filled with pure and recycled argon) to remove oxide films. Sodium and potassium from Merck were purified prior to use according to the procedure described elsewhere.[22,23] An alloy of nominal composition $Na_2K_2In_5Tl_3$ was prepared by melting together the elements in niobium reactors, lid-sealed by arc-welding in an argon atmosphere. It was heated up to 600 °C and homogenized, then allowed to cool slowly to room temperature at the rate of 4 °C h^{-1} for crystal growth. The air sensitive product was not homogeneous. Some crystals were selected from crushed bulk samples, inserted in Lindemann glass capillaries and then checked for singularity by oscillation and Weissenberg diffraction techniques. These preliminary analyses indicated that the crystals possess a trigonal symmetry. The best single crystal was selected and mounted on an Enraf-Nonius CAD-4 automatic diffractometer for data recording. Accurate lattice parameters were determined by least-squares refinement of the angular positions of 25 reflections collected and automatically centered on the diffractometer. Analysis of the single crystal by absorption flame spectroscopy indicated an atomic ratio Na : K : In : Tl of 1.71 : 2.63 : 7.50 : 1. After structure determination, a new synthesis was carried out starting from the ideal composition $Na_{12}K_{18}In_{53}Tl_7$; it gave a homogeneous and well-crystallized product whose X-ray powder pattern could be indexed on the basis of parameters from the investigated single crystal.

Structure solution and refinement

$Na_{12}K_{18}In_{53}Tl_7$ crystallizes in the $R\bar{3}m$ space group. Crystal data are summarized in Table 1. Integrated diffraction intensities of 4164 reflections were collected (Enraf-Nonius CAD-4 diffractometer, graphite-monochromated MoKα radiation, $\lambda = 0.71073$ Å) at room temperature within the $hk\bar{l}$ octant of the hexagonal cell. Scan times of 100 s were programmed. During data collection, the intensities of three standard reflections were checked after every hour and no significant loss was observed. Data were corrected for background and Lorentz polarization effects and, after the accurate composition was known, for absorption using the numerical procedure supplied by SHELX 76.[24] Intensities of equivalent reflections average well ($R_{ave} = 4.11\%$) in the $\bar{3}m$ Laue class. The structure was solved in the rhombohedral space group $R\bar{3}m$ by the direct methods of SHELXS 86.[25] Refinements have been carried out against intensities using the program SHELXL 93.[26] During the refinement, owing to some small temperature factors when refined with indium (too large when refined with thallium), it became obvious that indium and

Table 1 Crystallographic data for $Na_{12}K_{18}In_{53}Tl_7$

Compound	$Na_{12}K_{18}In_{53}Tl_7$
Formula weight	34022
System, space group	Rhombohedral, $R\bar{3}m$
Lattice parameters (Å)	$a = b = 16.846(3)$
	$c = 43.339(7)$
Volume/Å^3	10651.3
Z	4
μ(MoKα)/cm^{-1}	225.2
F(000)	14571
Diffractometer	Enraf Nonius CAD-4
Radiation	MoKα (0.7107 Å)
Octant	$h\bar{k}l$
θ_{max}/°	25
Scan type	$\omega-(4/3)\theta$
Temperature/K	293
Crystal dimensions/mm	0.2 × 0.1 × 0.05
Observed reflections, criterion	1462, $I > 3\sigma(I)$
Measured reflections	4164
Unique reflections, R_{ave} (%)	2277, 4.11
ρ_{calc}/g cm^{-3}	5.30
Transmission factors range	0.057–0.416
Final max/min in difference map/e Å^{-3}	−1.84, +2.06
Goodness-of-fit indicator	1.046
$R_1 = \Sigma\|\|F_o\| - \|F_c\|\|/\Sigma\|F_o\|$ (%)	3.61
$wR_2 = \{\Sigma[w(F_o^2 - F_c^2)^2]/\Sigma w(F_o^2)^2\}^{\frac{1}{2}}$ (%)	8.51
Weighting scheme	$1/[\sigma(F_o^2) + (0.044P)^2 + 309.56P]$ where $P = (F_o^2 + 2F_c^2)/3$

thallium were mixed at three atomic sites of the cluster framework. In a first step, each of these sites was refined independently from the others with fractional In/Tl occupations whose sum was constrained to unity, and positions of alkali metal atoms were deduced from subsequent Fourier syntheses. Refinement by full-matrix least-squares methods were first carried out using isotropic thermal parameters and the three relative In/Tl occupations allowed to vary together. Finally, all atomic positions were refined using anisotropic temperature factors. Multiplicity refinements of alkali metal atoms (U_is varying) with heavy atoms kept fixed, showed that K(2) and K(3) sites are not fully occupied, with deviations from unity of more than 7σ and 8σ [86(2) and 84(2)% occupations, respectively]. These occupations do not vary when heavy atoms are freed and, in these conditions, the Na/K ratio for the whole structure is 0.66(2). Refinement of these sites with mixed Na/K occupations (summing to unity) gives the same R factors owing to thermal factor adjustment, but leads to an overall Na/K ratio close to one and largely exceeding that determined analytically [0.65(1)]. Refinements of the structure in the lower space groups $R32$, $R\bar{3}$ or $R3$ could not overcome these occupational disorder problems and careful examination of the X-ray photographs, even after long exposure, did not show evidence for any multiple cell. The final refinement (121 parameters varied) leads to the stoichiometry $Na_{12}K_{18.15}In_{53.14}Tl_{6.86}$ that we will report, for convenience, as $Na_{12}K_{18}In_{53}Tl_7$.

CCDC reference number 440/027.

Results and Discussion

Structure description

The main bond distances are given in Table 2. The three-dimensional network of Group 13 elements contains icosahedra and 16-atom polyhedra (Fig. 2). Icosahedra (A and B) are located at sites 9(e) and 3(b) and display 2/m and $\bar{3}m$ symmetry, respectively. The 16-atom polyhedron (C) sits around the threefold axis [site 6(c), symmetry 3m] and is paired to a homolog through the $\bar{3}m$ inversion. Centers of icosahedra are

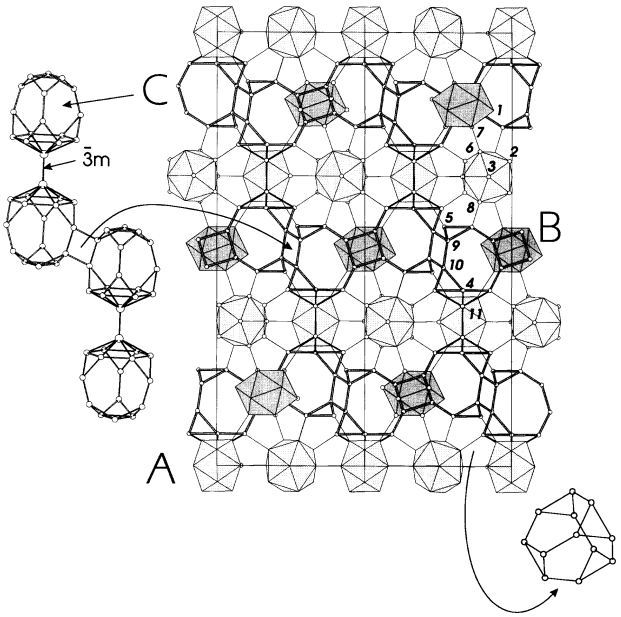

Fig. 2 [1$\bar{1}$0] projection of the $R\bar{3}m$ unit cell of $Na_{12}K_{18}In_{53}Tl_7$ displaying interconnected polyhedral units: icosahedra (shaded) and open 16-atom polyhedra (left). A 12-atom Friauf cavity is also shown (right). Numbering refers to triel atoms. For clarity, alkali cations have been omitted

disposed within a Kagomé network at the copper atom positions in the $MgCu_2$ Friauf–Laves structure,[27] while magnesium positions are occupied by polyhedra C.

Icosahedron A is bonded to six surrounding icosahedra (four A and two B), and to six 16-vertex polyhedra C. Icosahedron B is connected to six icosahedra A and has six non-*exo*-bonded apices. Coordination around icosahedron B is depicted in Fig. 3; noteworthy is the 72-atom outer coordination shell, with 38 faces (6 square, 6 pentagonal, 20 hexagonal and 6 heptagonal) and 108 edges, which satisfies the Euler relation $V + F = E + 2$ (V, F and E being the number of vertices, faces and edges). Polyhedron C is connected to nine icosahedra A, doubly bonded to three alike units around the threefold axis (see the 4c-8e square in Fig. 2) and paired to another one along the threefold axis.

The $Na_{12}K_{18}In_{53}Tl_7$ structure may be viewed as the packing of M_{72} building block cages centered on icosahedron B (Fig. 3). Each single cage is fused within the xy plane to six alike units by square-face-sharing. M_{72} spheres belonging to adjoining layers are not tangent, but wedged by icosahedron A. Layers are shifted by nearly 17.4 Å from each other along the [211] direction (Fig. 3).

This $R\bar{3}m$ structure can also be schematically described along the hexagonal c axis as an **ABABAB** packing in which **A** refers to an icosahedron A layer and **B** to a corrugated layer of icosahedra B plus polyhedra C. These two layers are connected through 2c–2e bonds involving vertices of adjoining polyhedra. Interpolyhedral voids (Friauf truncated tetrahedra), as well as the large 16-atom polyhedron (C) contain alkali cations.

The Tr—Tr bond lengths (Tr = In, Tl), as well as the A—Tr and A—A (A = K, Na) distances are quite similar to those usually found, with the exception of the K(4)—Na(4) distance of 3.429(7) Å, which is slightly below the shortest K—Na distances observed in other intermetallic systems (3.58–3.69 Å).[28,29]

Chemical bonding and electronic requirements

In this type of intermetallic phase, alkali metals occupy structural voids, generally in front of polyhedral faces forming a dual polyhedra (*e.g.* pentagonal dodecahedron around an

Table 2 Main interatomic distances (in Å) of less than 3.9 Å in $Na_{12}K_{18}In_{53}Tl_7$

Tl/In(1)		In(7)	3.053(2)			In(7)	3.708(4)
	2	In(7)	3.137(1)			In(6)	3.716(4)
	2	Tl/In(1)	3.277(1)			In/Tl(2)	3.733(4)
						In(8)	3.781(4)
In/Tl(2)		In(3)	3.026(2)			K(2)	3.802(6)
		In(3)	3.028(2)			Na(4)	3.87(1)
		In(8)	3.110(1)			In/Tl(4)	3.867(4)
		In/Tl(4)	3.122(2)				
		In(6)	3.125(1)	K(2)		Tl/In(1)	3.496(7)
		In/Tl(2)	3.164(3)		2	In/Tl(2)	3.502(4)
					2	In(6)	3.619(3)
In(3)		In(3)	2.856(2)		2	In/Tl(4)	3.620(3)
		In(3)	3.001(2)		2	In(7)	3.682(4)
		In/Tl(2)	3.026(2)		2	In(3)	3.690(6)
		In/Tl(2)	3.028(2)		2	K(1)	3.802(6)
		In(8)	3.044(2)				
		In(6)	3.049(2)	K(3)	2	In/Tl(2)	3.600(5)
					2	In/Tl(2)	3.606(5)
In/Tl(4)		In(10)	3.008(2)		2	In/Tl(4)	3.609(7)
		In/Tl(4)	3.081(2)		2	K(3)	3.680(4)
		In/Tl(2)	3.122(2)		2	In/Tl(4)	3.690(7)
		In/Tl(4)	3.222(2)		2	In(3)	3.770(4)
		Na(4)	3.53(1)				
		In(11)	3.544(2)	K(4)	3	Na(4)	3.429(7)
					3	In(10)	3.844(1)
In(5)		In(8)	2.929(2)				
	2	In(9)	2.956(2)	Na(1)	2	In(6)	3.428(3)
	2	In(5)	3.146(1)			In(6)	3.428(3)
					2	In(3)	3.51(1)
In(6)		In(7)	2.987(2)		2	In(3)	3.51(1)
		In(8)	2.991(1)		2	In(3)	3.51(1)
	2	In(3)	3.049(2)		2	In(7)	3.54(2)
	2	In/Tl(2)	3.125(1)			In(7)	3.54(2)
In(7)		In(6)	2.987(2)	Na(2)		In(10)	3.334(8)
	2	In(7)	3.025(1)			In(9)	3.37(1)
		Tl/In(1)	3.053(2)		2	In/Tl(2)	3.415(6)
	2	Tl/In(1)	3.137(1)		2	In(3)	3.506(9)
					2	In(8)	3.515(5)
In(8)		In(5)	2.929(2)		2	In(5)	3.678(7)
		In(6)	2.991(1)			Na(3)	3.739(8)
	2	In(3)	3.044(2)		2	In/Tl(4)	3.794(5)
	2	In/Tl(2)	3.110(1)				
				Na(3)	2	In(8)	3.400(3)
In(9)		In(10)	2.813(2)			In(8)	3.400(3)
	2	In(5)	2.956(2)		2	In(3)	3.53(1)
		In(10)	3.008(1)		2	In(3)	3.53(1)
					2	In(3)	3.53(1)
In(10)		In(9)	2.813(2)		2	In(5)	3.54(2)
	2	In/Tl(4)	3.008(2)			In(5)	3.54(2)
		In(9)	3.008(1)			Na(2)	3.739(8)
					2	Na(2)	3.739(8)
In(11)		In(11)	3.062(9)				
	6	In/Tl(4)	3.544(2)	Na(4)		Tl/In(1)	3.323(5)
						K(4)	3.429(7)
K(1)		In(9)	3.592(4)		2	In/Tl(4)	3.53(1)
		In(10)	3.627(4)			In(5)	3.54(1)
		Tl/In(1)	3.628(4)		2	In(9)	3.683(8)
		Tl/In(1)	3.673(4)		2	In(10)	3.718(6)
		In(5)	3.704(4)		2	K(1)	3.87(1)

icosahedron) or are encapsulated inside larger clusters as, for instance, the 16-atom icosioctahedra.[22] According to the Zintl–Klemm–Busmann concept,[30,31] it has been assumed that alkali metals donate their electron (solvating cations) in order to stabilize the electronegative element network. Parallel to the electron requirements, alkali cation sizes (size selectivity) and packing limitations play crucial roles in modelling these phases into a large variety of structures. Simple electron counting methods have proved very efficient in interpreting and rationalizing cluster framework formation.[2,6,9,10] For the icosahedron, Wade's rules predict a polyhedral count of 50 electrons (PEC) of which 26 are used in skeletal bonding, the 24 remaining electrons are left in nonbonding pairs or participate in *exo*-bonding within the cluster networks.

In the unit cell of $Na_{12}K_{18}In_{53}Tl_7$, there are nine twelvefold *exo*-bonded icosahedra (A), three sixfold *exo*-bonded icosahedra (B) and six open 16-atom polyhedra (C) of which all atoms are *exo*-bonded. According to Wade's rules, one can assume each icosahedron A to contribute 38 valence electrons to the bonding and each icosahedron B 44 electrons (26 skeletal, 6 *exo*-bonding and 12 nonbonding). The valence electron count (VEC) for an In_{16} pair has been determined by an extended Hückel calculation using the one-electron approximation[32] in which 30 In atoms have been saturated with hydrogen in order to simulate *exo*-bonding. In this $(In_{16}H_{15})_2$ unit, for which overlap populations are indicated for each bond type in Fig. 4, a closed shell is achieved with a polyhedral count of 150 electrons and an estimated HOMO–

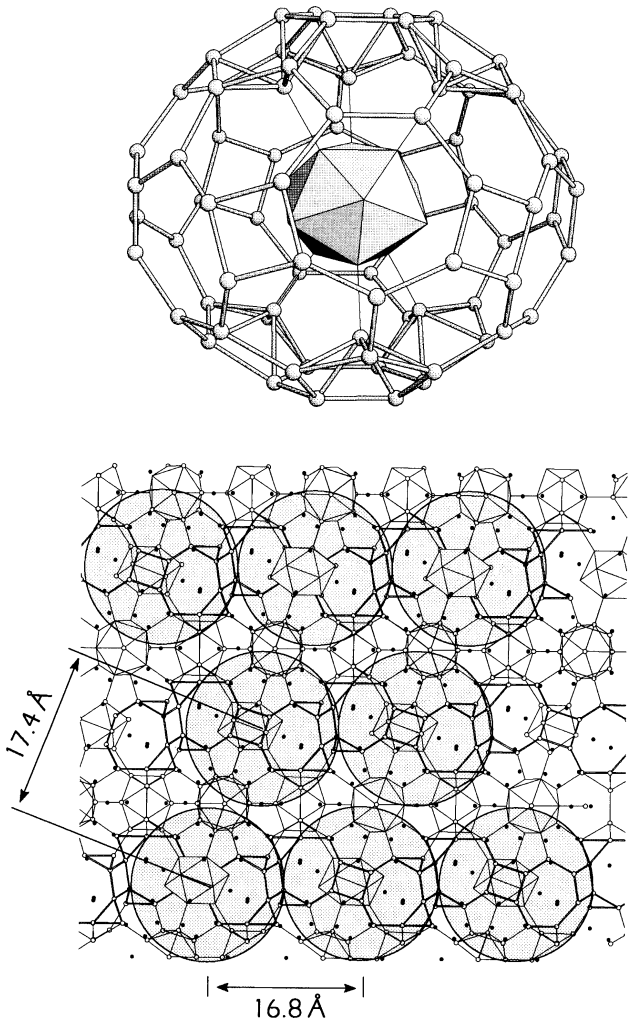

Fig. 3 (Top) The M_{72} coordination shell around icosahedron B in the $Na_{12}K_{18}In_{53}Tl_7$ structure. Top and bottom apices of the icosahedron are connected to atoms that cap the six pentagonal faces from the inside. (Bottom) Projection along the $[1\bar{1}0]$ direction of the $R\bar{3}m$ structure, emphasizing the layering of the M_{72} 'building block' bucky spheres

LUMO gap of 2.5 eV. This leads to 60 valence electrons for each In_{16} individual unit. In these conditions, the valence electron count required for the unit cell is 834 [9(A) × 38 + 3(B) × 44 + 6(C) × 60], instead of the 840.6 electrons given by the stoichiometry.

In order to have a more detailed understanding of this bonding problem, we have performed a band calculation[33] and a density of states (DOS) analysis.[34] These densities of states have been calculated with a set of 34 k points taken in the irreducible wedge of the Brillouin zone. Our calculations used an effective Hamiltonian of the extended Hückel type[35] with the parameters and exponents given in the appendix. The diagonal H_{ij} matrix elements were calculated by means of the modified Wolfsberg–Helmholz formula.[36] Band structure calculations have been carried out in the full energy domain with the rhombohedral primitive cell as the repeat unit. Except for one mixed In/Tl atomic site (corresponding to the six non-*exo*-bonded waist atoms of icosahedron B), which is occupied at 67% by thallium, other sites within the structure are fully or predominantly occupied by indium. Therefore, calculations can be easily simplified by using 6 Tl and 74 In atoms per primitive rhombohedral cell. Sodium and potassium atoms have been considered as electron donors and not taken into account in the calculations. Special paths in the Brillouin zone are depicted in Fig. 5.

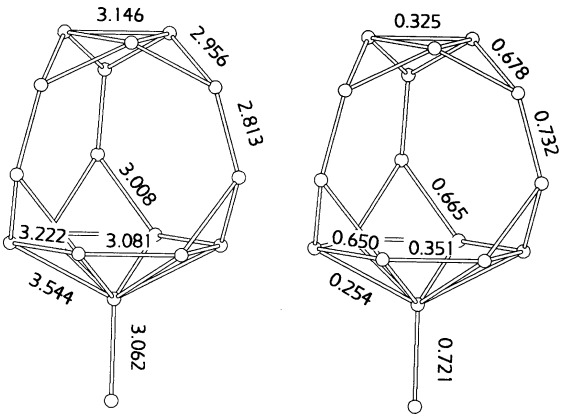

Fig. 4 Bond lengths (in Å, left) and overlap populations (right) within the open 16-atom polyhedron (C) in $Na_{12}K_{18}In_{53}Tl_7$

The calculated band structure for the three-dimensional network of $Na_{12}K_{18}In_{53}Tl_7$ is shown in Fig. 6 where, for clarity, the energy domain has been restricted to the range −8 to −3.5 eV. Dispersion curves are relatively flat, especially for the three bands lying around −5.2 and −5.8 eV. Crystal orbital analysis at the center of the BZ (point Γ) shows that practically only atoms in the sixfold *exo*-bonded icosahedron B contribute to these bands. Individual atomic orbital contributions to these a_{1g} and e_g (in symmetry D_{3d}) crystal orbitals are schematized in Fig. 6. Analysis of the projected densities of states shows that participation of the In and Tl s orbitals is very weak whereas the Tl 6p contribution is larger than that of In 5p (by nearly two times).

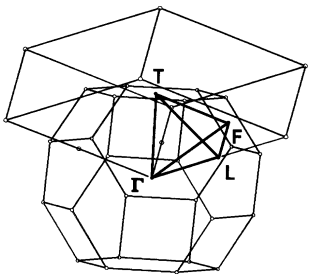

Fig. 5 The three-dimensional Brillouin zone of the primitive rhombohedral cell delimited by the special k points Γ (0, 0, 0), T ($\frac{1}{2}$, $\frac{1}{2}$, $\frac{1}{2}$), F ($\frac{1}{2}$, $\frac{1}{2}$, 0) and L ($\frac{1}{2}$, 0, 0)

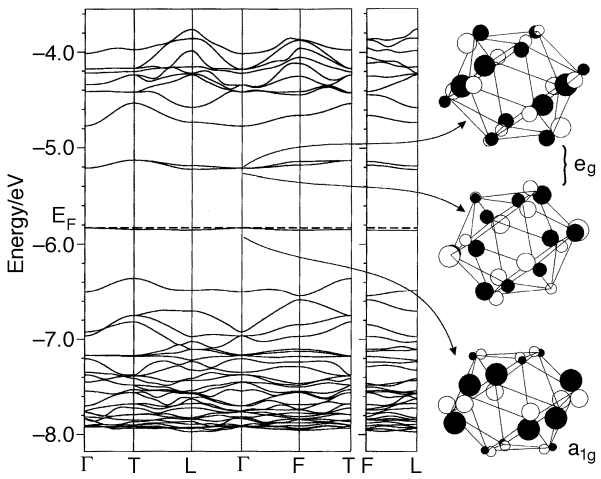

Fig. 6 Band structure for the $R\bar{3}m$ $Na_{12}K_{18}In_{53}Tl_7$ compound. Na and K atoms have been considered as one-electron donors and neglected in the calculation. The Fermi level (−5.83 eV) is indicated for 280 electrons (rhombohedral primitive unit). Schematic representations of the predominant atomic populations at point Γ are given (on the right) for the three crystal orbitals (a_{1g} and e_g)

The COOP[37] (crystal orbital overlap populations) values indicate that the crystal orbital near the actual Fermi level (a_{1g} at Γ) has a weak antibonding character as the result of antibonding (Tl—Tl, Tl—In) and bonding (In—In) interactions (see Table 3). The e_g level is readily antibonding and increasing the electron content to 282 (846 in the Bravais rhombohedral cell) would evidently destabilize the sixfold *exo*-bonded icosahedron B.

It is likely that this reduction (filling the levels up to −5.2 eV) would affect the compound by expulsing some of the non-*exo*-bonded atoms from icosahedron B. Such occurences have already been encountered in gallium phases,[9,10,38–41] where they lead to atomic defections within anionic networks and to formation of more electron-rich clusters (*nido*, *arachno*, *etc.*).

Filling levels up to the actual Fermi energy ($E_F = -5.83$ eV) with 280 electrons (formally 280.2 per primitive cell according to the refined stoichiometry) would lead to a closed-shell configuration. The two extra electrons, with regard to our previous estimate of 278, would almost exclusively fill icosahedron B (Tl_6In_6) states (mainly π antibonding at the Tl_6 waist). However, the temperature-dependent resistivity measurements (on single crystals, two-probe method, direct current 10–100 mA, range 223–333 K, ρ of the order of 2×10^{-3} Ω cm at 293 K) indicate a semiconducting behavior with a small activation energy (0.072 eV). There is an apparent contradiction between this low activation energy and the relatively large band gap (in Fig. 6). We would better consider the extra valence electrons as trapped in alkali metal states. In the primitive cell, there are two Na(4)—K(4) pairs with a distance of 3.43 Å, sufficiently short to raise the question on whether or not some bonding is to be considered between these atoms. Electron localization on these atomic pairs could reduce this contradiction. It is evident that theoretical investigations, at more a sophisticated level than the extended Hückel method, would be necessary for a better understanding of the problem.

Table 3 Calculated overlap populations within icosahedron B in $Na_{12}K_{18}In_{53}Tl_7$

Electron content	Tl—Tl	Tl—In	In—In
278	0.459	0.375	0.318
280	0.397	0.332	0.390
282	0.338	0.310	0.385
284	0.275	0.287	0.380

Relation to the C15 ($MgCu_2$) family

The crystal structure examined in this work and those of parent phases containing Group 13 elements exemplify the versatility of triels to aggregate within different cluster networks according to the electronic and packing requisites. As the term *icosogen* has been used by King[8] to characterize Group 13 elements, it is not surprising for a stable icosahedral cluster to be the most frequent building block occurring within these cluster frameworks. The Tr_{12} are linked together, mostly by (2c–2e) bonds between vertices of adjacent units. Whereas icosahedral symmetry can propagate in long range or aperiodic structures (quasicrystals), provided that some lattice distortions occur, in periodic three-dimensional networks extended icosahedral symmetry may be observed but is limited to a few shells around an 'icosahedral seed'. The five-fold symmetry propagation within the 6D icosahedral space is frozen by inclusion of spacer units, which can be smaller (isolated atoms, triangles …) or larger (15-, 16-, 17-vertex or more complex polyhedra). Within the icosogen Ga, In and Tl triad, cluster network formation and stabilization depends upon the subtle balance between the number of available electrons and the sizes of triels and alkali cations. The latter occupy voids (*e.g.* Friauf polyhedra, see Fig. 2) between empty icosahedral clusters and also fill larger spacers.

There are some logical links between these phases, depending upon the criteria put forward: electron concentration, packing limitations and sterical strain, as well as electronegativities, especially when heteroelements are present within the anionic network.

All phases reported in Table 4 can be described in a primitive rhombohedral cell; α is equal to 60° for the cubic *Fd*3*m*, but differs more or less from 60° for the $R\bar{3}m$ phases. In all structures, icosahedron centers are arranged on a Kagomé network at the copper atom positions in the $MgCu_2$ structure type, the Mg sites being hierarchically occupied by other polyhedra that have been previously referred to as 'spacers'.[6] These spacers are the 15- or 16-atom open polyhedra in the more reduced rhombohedral phases (top of Table 4), the regular (deltahedral) icosioctahedron in cubic phases and the condensed 'triply fused (by face sharing) icosahedron (M_{28})' in the less reduced rhombohedral phases (bottom of Table 4). There is a close relationship (Fig. 7) between the open 16-atom and 15-atom polyhedra; the latter results from removal of the atom that caps the hexagonal face of the 16-atom cluster but keeps the same number of skeletal electrons (44). According to local symmetries, spacers are con-

Table 4 Selected features of the anionic networks, hierarchically related to the C15 Friauf–Laves structure type ($MgCu_2$), in some alkali metal/early post-transition element phases

Compound	Space group	Angle of the primitive rhombohedral cell	Anionic mean charge per heavy atom	Atomic units or clusters forming the anionic network
Na_7Ga_{13} [50]	$R\bar{3}m$	57.36	−0.538	Ga_{12}, Ga_{15}
$K_{21.33}In_{39.67}$ [28]	$R\bar{3}m$	57.53	−0.538	In_{12}, In_{15}
$Na_{12}K_{18}In_{53}Tl_7$	$R\bar{3}m$	57.85	−0.504	$(In/Tl)_{12}$, $(In/Tl)_{16}$
$Na_{36}Ag_7Ga_{73}$ [51]	*Fd*3*m*	60	−0.450	Ga_{12}, Ag_4Ga_{12}
$Li_{18}Cu_5In_4Ga_{31}$ [52]	*Fd*3*m*	60	−0.450	$(Cu/Ga)_{12}$, In_4Ga_{12}
$Na_{35}Cd_{24}Ga_{56}$ [22]	*Fd*3*m*	60	−0.438	Ga_{12}, $Cd_{12}Ga_4$
$Na_{17}Ga_{29}In_{12}$ [53,54]	*Fd*3*m*	60	−0.415	In_{12}, $In_{12}Ga_5$
$K_{17}In_{41}$ [53,54]	*Fd*3*m*	60	−0.415	In_{12}, In_{17}
$Na_{13}K_4Ga_{47.45}$ [55]	$R\bar{3}m$	65.77	−0.358	Ga_{12}, Ga_{28}
$Na_{21}K_{14}Cd_{17}Ga_{82}$ [56]	$R\bar{3}m$	65.03	−0.354	$(Ga/Cd)_{12}$, $(Ga/Cd)_{28}$
$Na_{13}K_4Ga_{49.57}$ [42]	$R\bar{3}m$	65.54	−0.343	Ga_{12}, Ga_{28}
$Na_{17}Cu_6Ga_{46.5}$ [43]	$R\bar{3}m$	65.30	−0.324	$(Ga/Cu)_{12}$, {Cu, $2(Ga/Cu)_{28}$}
$Na_{17}Zn_{12}Ga_{40.5}$ [44]	$R\bar{3}m$	65.72	−0.324	$(Ga/Zn)_{12}$, {Zn, $2(Ga/Zn)_{28}$}
$Na_{34}Cu_6Cd_7Ga_{92}$ [57]	$R\bar{3}m$	65.54	−0.324	Ga_{12}, $(Ga/Cd)_{12}$, {Cu, $2(Ga_{25}Cu_3)$}
$K_{34}Zn_{20}In_{85}$ [58]	$R\bar{3}m$	65.24	−0.324	In_{12}, $Zn_{10}In_{18}$

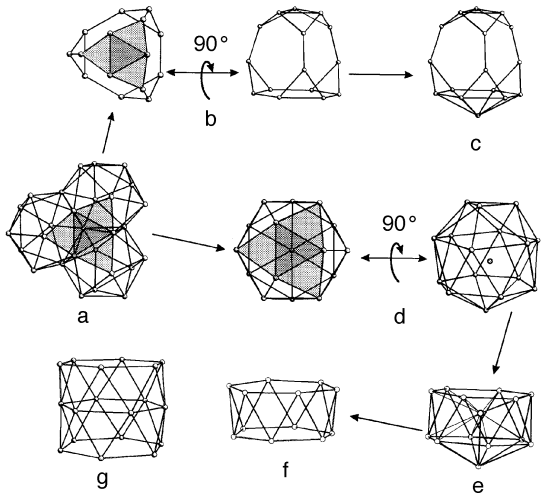

Fig. 7 Representation of various spacers within some icosahedron-based frameworks: (a) triply fused icosahedron, (b) open 15-vertex polyhedron, (c) open 16-vertex polyhedron, (d) icosioctahedron, (e) collapsed 14-atom polyhedron, (f) antiprismatic hexagonal M_{12} ('drum'), (g) triple-decker M_{18} tubular cluster

nected to alike units within different bonding patterns. In cubic phases, the icosioctahedron is tetrahedrally linked to four icosioctahedra by 2c–2e bonds (Fig. 8). The open M_{15} spacer in $R\bar{3}m$ phases is doubly linked to three alike units around the threefold axis, but not interconnected along it as is the M_{16} spacer. The triply fused icosahedron is not interconnected along the threefold axis in $Na_{13}K_4Ga_{49.57}$ [42] (Fig. 8) but forms a sandwich unit ($M_{28}NM_{28}$) in $Na_{17}Cu_6Ga_{46.5}$ [43] and $Na_{17}Zn_{12}Ga_{40.5}$ [44] by incorporating a heteroatom at the $\bar{3}m$ center. The wide (but flattened) triply fused icosahedron fills voids between icosahedra, more efficiently allowing full *exo*-bonding of the icosahedron at site 3(*b*), which is only sixfold *exo*-bonded when associated with the more reduced open 15- and 16-atom spacers. Furthermore, it is worth noting that for structures containing triply fused icosahedra, the lower level of reduction (less solvating alkali counter cations) is responsible for contraction of the rhombohedral cell ($\alpha > 60°$), while in more reduced phases including more alkali counter cations, the rhombohedral cell is elongated ($\alpha < 60°$).

Previous calculations[6] have shown the triply fused icosahedron to be stabilized with 62 skeletal electrons, the open 15- and 16-atom polyhedra with 44 and the regular (deltahedral) icosioctahedron with 36 skeletal electrons. There are striking resemblances not only between the phases discussed above, but also with some other phases that cannot be derived so simply from the C15 structural family. One wonders whether some 'chemical surgery' inside the triply fused icosahedron would supply the M_{15}, M_{16} and centered, or empty, icosioctahedron (Fig. 7). The latter would transform into the collapsed M_{14} cluster like that recently found in $K_{49}Tl_{108}$;[45] EH calculations show it to be stabilized with 32 skeletal electrons. From that, removal of the central and hexagon capping atom leads to the more classical hexagonal antiprismatic M_{12} cluster found in $A_3Na_{26}In_{48}$ (A = K, Rb, Cs),[46,47] (30 skeletal electrons). At last, condensation of two M_{12} units would give the triple-decker M_{18} illustrated by the $Cd_{12}In_6$ tubular cluster recently found in the $Na_8K_{23}Cd_{12}In_{48}$ hexagonal phase.[21]

These findings, once again, illustrate the remarkable ability of the triel elements to form some interesting cluster frameworks and to organize within a structural family, depending on the subtle balance between atomic sizes, electron supply, packing contingencies and electronegativity differences.

Acknowledgements

The authors thank Martin Köckerling for having kindly provided to them a PC adaptation of the EHT band calculation program.

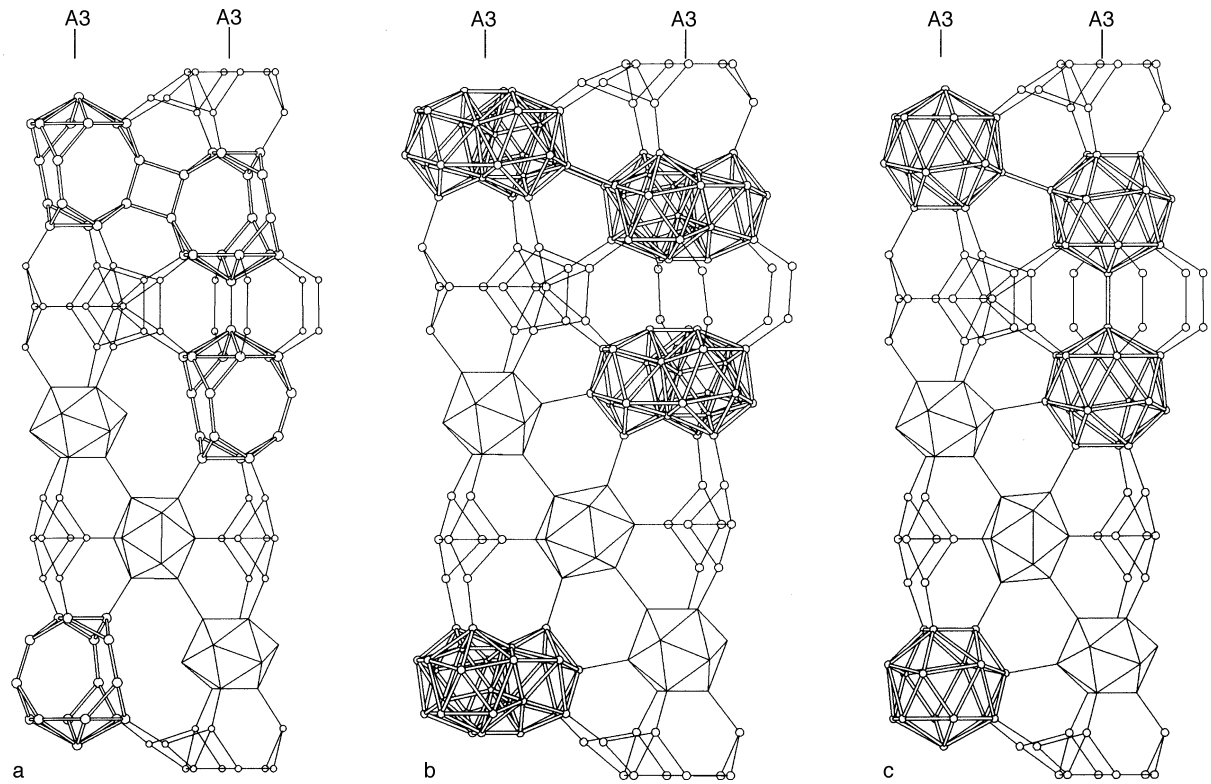

Fig. 8 Cluster layering within the (a) $R\bar{3}m$ $Na_{12}K_{18}In_{53}Tl_7$, (b) $R\bar{3}m$ $Na_{13}K_4Ga_{49.57}$ and (c) $Fd3m$ $Na_{35}Cd_{24}Ga_{56}$ structures

Appendix

Exponents and parameters used in the calculations

Atom	Orbital	H_{ii}/eV	ξ
In[a]	5s	−12.60	1.90
	5p	−6.19	1.68
Tl[b]	5s	−16.20	2.37
	5p	−9.00	1.97

[a] From ref. 48. [b] From ref. 49.

References

1 W. Blase, G. Cordier and M. Somer, *Z. Kristallogr.*, 1991, **194**, 150.
2 J. D. Corbett, in *Chemistry, Structure and Bonding in Zintl Phases and Ions*, ed. S. Kauzlarich, VCH, New York, 1996, ch. 3.
3 D. A. Hansen and J. F. Smith, *Acta Crystallogr.*, 1967, **22**, 836.
4 G. Cordier and V. Müller, *Z. Kristallogr.*, 1992, **198**, 281.
5 G. Cordier and V. Müller, *Z. Naturforsch., B*, 1994, **49**, 935.
6 C. Belin and M. Tillard-Charbonnel, *Prog. Solid State Chem.*, 1993, **22**, 59.
7 K. Wade, *Adv. Inorg. Chem. Radiochem.*, 1976, **18**, 1.
8 R. B. King, *Inorg. Chem.*, 1989, **28**, 2796.
9 J. K. Burdett and E. Canadell, *J. Am. Chem. Soc.*, 1990, **112**, 7207.
10 J. K. Burdett and E. Canadell, *Inorg. Chem.*, 1991, **30**, 1991.
11 D. M. P. Mingos, *J. Chem. Soc., Chem. Commun.*, 1983, 706.
12 M. Zhao and B. M. Gimarc, *Inorg. Chem.*, 1993, **32**, 4700.
13 R. Hoffmann, *Angew. Chem., Int. Ed. Engl.*, 1987, **26**, 846.
14 H. G. von Schnering, R. Hector, C. Gil, W. Hönle, A. Burkhardt, G. Krier and O. K. Andersen, *Angew. Chem., Int. Ed. Engl.*, 1995, **34**, 103.
15 R. Llusar, A. Beltran, J. Andres, S. Silvi and A. Savin, *J. Phys. Chem.*, 1995, **99**, 12483.
16 E. Canadell and M. H. Whangbo, *Chem. Rev.*, 1991, **91**, 965.
17 W. Müller and J. Stöhr, *Z. Naturforsch., B*, 1977, **32**, 631.
18 J. Stöhr and H. Schäfer, *Z. Anorg. Allg. Chem.*, 1981, **474**, 221.
19 M. Tillard-Charbonnel, C. Belin and J. L. Soubeyroux, *Eur. J. Solid State Inorg. Chem.*, 1990, **27**, 759.
20 M. Tillard-Charbonnel, C. Belin, A. Manteghetti and D. Flot, *Inorg. Chem.*, 1996, **35**, 2583.
21 D. Flot, M. Tillard-Charbonnel and C. Belin, *J. Am. Chem. Soc.*, 1996, **118**, 5229.
22 M. Tillard-Charbonnel and C. Belin, *Mater. Res. Bull.*, 1992, **27**, 1277.
23 M. Tillard-Charbonnel, N. Chouaibi and C. Belin, *C. R. Séances Acad. Sci. Paris*, série II, 1990, **69**, 311.
24 G. M. Sheldrick, *SHELX-76, Program for Crystal Structure Determination*, University of Cambridge, Cambridge, UK, 1976.
25 G. M. Sheldrick, *SHELXS-86, Program for Crystal Structure Solution*, Göttingen University, Göttingen, Germany, 1986.
26 G. M. Sheldrick, *SHELXL-93, Program for Crystal Structure Refinements*, Göttingen University, Göttingen, Germany, 1993.
27 J. B. Friauf, *J. Am. Chem. Soc.*, 1927, **49**, 3107.
28 W. Carillo-Cabrera, N. Caroca-Canales and H. G. von Schnering, *Z. Anorg. Allg. Chem.*, 1994, **620**, 247.
29. Z. Dong and J. D. Corbett, *J. Am. Chem. Soc.*, 1994, **116**, 3429.
30 W. Klemm and E. Busmann, *Z. Anorg. Allg. Chem.*, 1963, **319**, 297.
31 H. Schäfer, B. Eisenmann and W. Müller, *Angew. Chem., Int. Ed. Engl.*, 1973, **12/9**, 694.
32 J. Howell, A. Rossi, D. Wallace, K. Haraki and R. Hoffmann, Quantum Chemistry Program Exchange (QCPE), Program No. 344, Forticon 8, Cornell University, Ithaca, NY, USA, 1977.
33 M. H. Whangbo and R. Hoffmann, *J. Am. Chem. Soc.*, 1978, **100**, 6093.
34 R. Hoffmann, *Angew. Chem., Int. Ed. Engl.*, 1987, **26**, 846.
35 R. Hoffmann, *J. Chem. Phys.*, 1963, **39**, 1397.
36 J. Ammeter, H.-B. Bürgi, J. Thiebeault and R. Hoffmann, *J. Am. Chem. Soc.*, 1978, **100**, 3686.
37 T. Hughbanks and R. Hoffmann, *J. Am. Chem. Soc.*, 1983, **105**, 1150.
38 M. Charbonnel and C. Belin, *Nouv. J. Chim.*, 1984, **8**, 595.
39 M. Charbonnel and C. Belin, *J. Solid State Chem.*, 1987, **67**, 210.
40 M. Tillard-Charbonnel, A. Chahine and C. Belin, *Z. Kristallogr.*, 1994, **209**, 280.
41 M. Tillard-Charbonnel, A. Chahine and C. Belin, *Mater. Res. Bull.*, 1993, **28**, 1285.
42 C. Belin and M. Charbonnel, *J. Solid State Chem.*, 1986, **64**, 57.
43 M. Tillard-Charbonnel, N. Chouaibi, C. Belin and J. Lapasset, *J. Solid State Chem.*, 1992, **100**, 220.
44 M. Tillard-Charbonnel, N. Chouaibi and C. Belin, *C.R. Acad. Sci. Paris*, série II, 1992, **315**, 661.
45 G. Cordier and V. Müller, *Z. Naturforsch., B*, 1993, **48**, 1035.
46 S. C. Sevov and J. D. Corbett, *Inorg. Chem.*, 1993, **32**, 1612.
47 W. Carillo-Cabrera, N. Caroca-Canales, K. Peters and H. G. von Schnering, *Z. Anorg. Allg. Chem.*, 1993, **619**, 1556.
48 C. Janiak and R. Hoffmann, *J. Am. Chem. Soc.*, 1990, **112**, 5924.
49 D. B. Kang, D. Jung and M. H. Wanghbo, *Inorg. Chem.*, 1990, **29**, 257.
50 U. Franck-Cordier, G. Franck-Cordier and H. Schäfer, *Z. Naturforsch., B*, 1982, **37**, 119.
51 M. Tillard-Charbonnel, A. Chahine and C. Belin, *Z. Kristallogr.*, 1993, **208**, 372.
52 A. Chahine, M. Tillard-Charbonnel and C. Belin, *Z. Kristallogr.*, 1995, **210**, 80.
53 G. Cordier and V. Müller, *Z. Kristallogr.*, 1993, **205**, 133.
54 G. Cordier and V. Müller, *Z. Kristallogr.*, 1993, **205**, 353.
55 D. Flot, L. Vincent, M. Tillard-Charbonnel and C. Belin, *Acta Crystallogr., Sect. C*, 1998, **54**, 174.
56 D. Flot, L. Vincent, M. Tillard-Charbonnel and C. Belin, *Z. Kristallogr.*, 1997, **212**, 509.
57 A. Chahine, M. Tillard-Charbonnel and C. Belin, *Z. Kristallogr.*, 1994, **209**, 542.
58 G. Cordier and V. Müller, *Z. Naturforsch., B*, 1995, **50**, 23.

Received in Montpellier, France, 5th September 1997;
Paper 7/08761F